Crystalline Adducts of Tetrakis(triphenylacetato)dichromium(II) with Benzene, Pyridine, and Diethyl Ether. Benzene as a Multiple π Donor

F. Albert Cotton,* Xuejun Feng, Piotr A. Kibala, and Marek Matusz

Contribution from the Department of Chemistry and Laboratory for Molecular Structure and Bonding, Texas A&M University, College Station, Texas 77843. *Received September 11, 1987*

Abstract: Three crystalline compounds, $Cr_2(O_2CCPh_3)_4 \cdot C_6H_6$ (**1**), $Cr_2(O_2CCPh_3)_4 \cdot Py$ (**2**), and $Cr_2(O_2CCPh_3)_4 \cdot 2Et_2O$ (**3**), have been prepared and structurally characterized. Compound **1** is obtained by reaction of $(\eta^5\text{-}C_5H_5)_2Cr$ with Ph_3CCO_2H in toluene/benzene, and the others are derived by recrystallization in the presence of pyridine and Et_2O, respectively. Crystallographic parameters are as follows. Compound **1**: tetragonal space group $P4/ncc$; $a = b = 20.787$ (4) Å, $c = 17.710$ (3) Å, $V = 7653$ (3) Å^3, and $Z = 4$. Compound **2**: tetragonal space group $I\bar{4}$, $a = b = 18.268$ (4) Å, $c = 10.919$ (2) Å, $V = 3644$ (2) Å^3, and $Z = 2$. Compound **3**: monoclinic space group $C2/c$; $a = 21.535$ (5) Å, $b = 17.065$ (5) Å, $c = 20.498$ (4) Å, $\beta = 90.65$ (3)°, $V = 7532$ (3) Å^3, and $Z = 4$. The $Cr_2(O_2CCPh_3)_4$ molecules pack in ways that are heavily influenced by the requirements of the CPh_3 groups, and this leaves holes of intermediate size in the axial regions of the $Cr_2(O_2CR)_4$ molecules. In **1** there is a benzene molecule centered in each hole so that the center of the benzene ring is 3.30 Å from each adjacent Cr atom, with the ring plane perpendicular to the Cr_2 axes. Calculations by the Xα-SW-SCF method show that the e_{1u} orbitals of the benzene molecules donate appreciable electron density to the π^* orbitals of the Cr_2 units, thus weakening the Cr–Cr bond, which has a length of 2.256 (4) Å. In the pyridine compound **2** the size of the cavity available allows only one pyridine molecule and also enforces a tilt relative to the Cr–Cr axis. The Cr–N distance is 2.31 (4) Å, and the Cr–Cr distance is 2.383 (4) Å. Each pyridine molecule is disordered systematically over four positions. In the ether-containing compound, two ether molecules are accommodated in each cavity, and thus each dichromium molecule has an axial Cr–O bond, 2.30 (1) Å, at each end and a Cr–Cr distance of 2.303 (4) Å.

One of the most challenging problems in the field of multiple bonds between metal atoms has been to identify and prioritize the factors that influence the strength of the quadruple interaction between the metal atoms in compounds containing the Cr_2^{4+} unit. Since reviews of the problem have been published,[1,2] it will not be necessary here to do more than note a few key points in order to place the new work that we are reporting in context.

In the type of compound we are considering there are two kinds of ligands, as shown schematically in I. The bridging ligands,

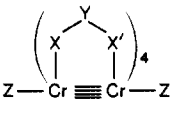

I

X–Y–X′, all four of which are usually the same, form Cr–X and Cr–X′ bonds called equatorial bonds; the X–Y–X′ ligands may be called equatorial ligands. The Cr–Z bonds are called axial bonds and the Z ligands axial ligands. It is generally accepted that both the equatorial ligands and the axial ligands influence the strength of the Cr-to-Cr interaction, but there has been disagreement as to the relative importance of these two kinds of ligands. We believe that the overwhelmingly most critical factor is whether axial coordination occurs or not, in the sense that, whatever the nature of the X–Y–X′ ligands, the Cr–Cr distance will be short (<2.0 Å) when there is *no* axial coordination and long (≫2.0 Å) when axial bonds are formed.

There is incontrovertible evidence for this view for those compounds in which the equatorial ligands are amidato ions. For all such compounds the Cr–Cr distances are ≤1.95 Å when axial ligands are absent, whereas the introduction of axial ligands causes increases (proportional to the number and basicity of the axial ligands) in the Cr–Cr distance to as much as 2.35 Å in a diyridine compound.

It is with the $Cr_2(O_2CR)_4$ compounds that the question has been most difficult to address experimentally. Even when these compounds are deprived of exogenous axial ligands, they form axial bonds in the crystalline state by intermolecular association, and to date no way of preventing this has been found. Hence, all Cr–Cr distances in crystalline $Cr_2(O_2CR)_4$ compounds have been found ≥2.28 Å, the distance in the crystalline, unsolvated acetate. It has been asserted by some that these long Cr–Cr distances in $Cr_2(O_2CR)_4$ compounds are mainly a consequence of the electronic properties of the RCO_2^- ligands and only secondarily traceable to the axial bonds. However, the experimental demonstration (by electron diffraction) that isolated molecules of $Cr_2(O_2CMe)_4$ in the gas phase have a Cr–Cr distance of 1.97 (1) Å refutes this and shows the primacy of the axial ligands in determining the strength of the Cr$\frac{4}{}$Cr bond.

Unfortunately, dichromium tetraacetate would appear to be the only $Cr_2(O_2CR)_4$ compound suitable for study by electron diffraction in the gas phase. While other types of experiment capable of providing structural data on $Cr_2(O_2CR)_4$ molecules in the absence of axial bonding would be desirable, they are not easy to envision. The most obvious possibility, in principle, would be to employ an R group that will promote a mode of crystal packing in which there are neither exogenous axial ligands nor intermolecular axial interactions between $Cr_2(O_2CR)_4$ molecules. In practice, because the R group is so far from the axial region of the molecule, direct blocking of the axial region by a bulky R group is not a promising approach. There is, however, the possibility that very bulky R groups, even though they do not block the axial positions of the molecule to which they belong, might lead to a form of crystal packing where the $Cr_2(O_2CR)_4$ molecules cannot associate with each other. If such a compound could then be crystallized from a noncoordinating solvent, a crystalline compound containing $Cr_2(O_2CR)_4$ molecules with no axial coordination might be obtained.

The present work was undertaken partly on the basis of this general idea. However, a somewhat more positive reason for choosing as the particular bulky R group $C(C_6H_5)_3$ was supplied by some exploratory work carried out earlier in this laboratory.[4] In this earlier work the compound $Mo_2(O_2CCPh_3)_4 \cdot THF$ was prepared and crystallized from THF. The structure was solved and partially refined. It showed a packing arrangement which

(1) Cotton, F. A.; Walton, R. A. *Multiple Bonds between Metal Atoms*; John Wiley and Sons: New York, 1982; Chapter 4.
(2) Cotton, F. A.; Walton, R. A. *Struct. Bonding* **1985**, *62*, 1.
(3) Cotton, F. A.; Ilsley, W. H.; Kaim, W. *J. Am. Chem. Soc.* **1980**, *102*, 3464.
(4) E. S. Shamshoum, unpublished work.

0002-7863/88/1510-2807$01.50/0

seemed to be controlled by the steric requirements of the CPh_3 groups and which resulted in there being very long intermolecular distances between the axial regions of adjacent molecules, with no O → Mo axial bonding of the type found in other unsolvated $Mo_2(O_2CR)_4$ compounds. Our hope was that if, indeed, the steric requirements of the bulky CPh_3 groups controlled the crystal packing, then it might be possible to obtain a similar crystal structure for the $Cr_2(O_2CCPh_3)_4$ compound, employing a noncoordinating solvent such as benzene. If this were to be successful, we would then have the opportunity to examine by X-ray crystallography the structure of a $Cr_2(O_2CR)_4$ molecule having no axial bonding.

As will now be explained, this is not how the results came out. Instead, we have encountered some novel types of axial interactions which are regulated by the packing relationships between the $Cr_2(O_2CCPh_3)_4$ molecules in the crystals. The major observation from the point of view of the Cr–Cr bond is that both σ and π interactions of this bond with the π orbitals of benzene rings can be shown to occur and to affect the length of the Cr–Cr bond.

Experimental Section

Bis(cyclopentadienyl)chromium, sublimed grade, was purchased from Strem Chemical Company, and triphenylacetic acid was purchased from Aldrich Chemical Company; both were used as received. All manipulations were done with the rigorous exclusion of oxygen and water in standard Schlenkware. All solvents were dried and freshly distilled under nitrogen.

Dichromium Tetrakis(triphenylacetate). Preparation of a Benzene Adduct. In a typical preparation 0.12 g (0.66 mmol) of bis(cyclopentadienyl)chromium and 0.32 g (1.1 mmol) of triphenylacetic acid were suspended in a 1:1 mixture of toluene and benzene. The reaction mixture was stirred at room temperature for 3 days, by which time the yellow precipitate of the product was deposited, usually in quantitative yield based on triphenylacetic acid. We use excess of chromocene, which is soluble in the solvents used in the reaction and can be easily separated from the product. The reaction mixture was filtered, the solid residue was washed with a small amount of benzene, and the product was vacuum dried. Single crystals for the X-ray diffraction experiments were prepared by following a slightly modified procedure. Triphenylacetic acid, 0.32 g (1.1 mmol), was suspended in 10–15 mL of benzene. A solution of 0.1 g (0.55 mmol) of bis(cyclopentadienyl)chromium in 10 mL of toluene was layered on top of the benzene suspension. A slow diffusion process took place, and in 2–4 weeks large (up to 2 mm), well-formed crystals of $Cr_2(O_2CCPh_3)_4 \cdot C_6H_6$ grew inside the Schlenk tube.

Preparation of Axial Adducts of Dichromium Tetrakis(triphenylacetate). The benzene molecule in the benzene adduct can be easily replaced by a variety of σ donating ligands.

Diethyl Ether Adduct. A freshly prepared sample of $Cr_2(O_2CCPh_3)_4 \cdot C_6H_6$ (0.1–0.2 g) was dissolved in CH_2Cl_2 to give a yellow solution. This was filtered through a short Celite bed into a narrow Schlenk tube. About 15 mL of 1,2-dichloroethane was layered on top of it followed by 5 mL of diethyl ether. Dichloroethane forms an interface that allows slow diffusion of diethyl ether into the dichloromethane solution. A crop of red crystals was collected after several days.

Pyridine Adduct. A freshly prepared sample of $Cr_2(O_2CCPh_3)_4 \cdot C_6H_6$ was dissolved in a benzene–pyridine mixture (5:1) to give a pale pink solution. This was filtered through a short Celite column and layered with hexane. Pale pink crystals were deposited during several days.

Other Adducts. Use of H_2O, MeOH, EtOH, and ammonia led to decompsotion of $Cr_2(O_2CCPh_3)_4$. Crystalline products were obtained with THF and pyrazine, but the crystals were not suitable for X-ray diffraction studies.

X-ray Crystallography. All crystals in this study were mounted in thin-walled capillaries filled with a mineral oil–mother liquor mixture (5:1). This was usually sufficient to prevent crystal decomposition due to solvent loss. Axial lengths and Laue class were always confirmed with oscillation photographs. Face (ab) diagonals were also photographed to confirm correct choice of axis for tetragonal cells. Body centering, when appropriate, was confirmed by photographing the body diagonal and comparing calculated and observed axial lengths. For the data collected with Mo radiation no absorption correction was applied (ψ scans of selected reflections did not show any significant variation in intensity). Data collected with Cu radiation were corrected for absorption with ψ scans. All data were processed by procedures routine to our laboratory.[5] Lorentz and polarization corrections were applied as well as decay corrections where applicable. All the relevant crystallographic data is summarized in Table I.

Structure Solution and Refinement. $Cr_2(O_2CCPh_3)_4 \cdot C_6H_6$. The data showed a rapid decline in intensity at high 2θ angles. The data were collected on a P3 autodiffractometer with a very low scan speed of 0.5°/min to optimize measurement of weak reflections. The structure was solved with the direct methods part of the SHELXS-86 package, which revealed a large part of the structure. This solution was also consistent with a Patterson map. The early stages of refinement proceeded with difficulty, and the two independent Cr–O and C–O distances were heavily correlated. Only after all the carbon atoms in the phenyl groups were found did the structure begin to refine efficiently. The benzene molecule was then located in a difference Fourier map, lying halfway between dichromium units with the benzene plane perpendicular to the Cr–Cr vector. The structure was refined isotropically with no constraints on the phenyl rings, which behaved well (acceptable bond distances, bond angles and thermal parameters). Because of the low number of observed data, anisotropic refinement was conducted with phenyl rings constrained to be perfectly hexagonal. All of the non-hydrogen atoms in the chromium molecule were refined anisotropically. Hydrogen atoms were added in the calculated positions with a single thermal parameter for all of them included in the refinement. The interstitial molecule of benzene was refined isotropically. A final review of the data showed some bad reflections with observed intensities higher than calculated. Seven of those were rejected from the data file (possible multiple reflections). The refinement converged to $R = 0.0681$ and $R_w = 0.0828$ for 589 reflections with $F_o^2 > 3\sigma(F_o)^2$ and 175 parameters refined (data to parameter ratio 3.36).

A second data set on $Cr_2(O_2CCPh_3)_4 \cdot C_6H_6$ was collected with Cu radiation. This data set, which was collected on the same crystal used for the Mo data, gave 858 (versus 589) reflections with $F_o^2 > 3\sigma(F_o)^2$. Because of the larger number of observed data available we decided to change the model and refine the phenyl rings freely. All the atoms of the dichromium molecule were refined anisotropically. Hydrogen atoms were added at the calculated distances, with a common thermal parameter included in the refinement. The benzene molecule was again refined isotropically. The six worst reflections were rejected from the data set. The final agreement factors were $R = 0.0640$ and $R_w = 0.0805$, with a data-to-parameter ratio of 4.06. In neither of these two refinements did we encounter any systematic disorder, which the rapid falloff of the reflection intensity at higher 2θ angles might have implied. This falloff can doubtlessly be attributed to loose packing dictated by the globular shape of the dichromium unit, and the large thermal parameters of all the phenyl carbon atoms (ca. 10 Å^2) and hydrogen atoms (ca. 15 Å^2) is indicative of this.

$Cr_2(O_2CCPh_3)_4 \cdot 2Et_2O$. This structure was also solved by the direct methods program provided by the SHELXS-86. Additional least-squares cycles and difference Fourier maps revealed the positions of the remaining atoms. There was a partial disorder of the carbon atoms of the ethyl groups in one of the ether molecules, which was modelled successfully (the disordered carbon atoms were assigned half occupancy). Phenyl groups were again constrained to be hexagons. Hydrogen atoms were added to the phenyl rings at the calculated distances, assigned a common thermal parameter, and included in the refinement. The dichromium unit was refined anisotropically. Axial ether molecules were refined isotropically with the exception of the oxygen atoms which were treated anisotropically. In the final cycle of the refinement 1878 data with $F_o^2 > 3\sigma(F_o)^2$ were used to refine 366 parameters, and the residuals were $R = 0.079$ and $R_w = 0.0837$. As before, phenyl groups showed large thermal motions.

$Cr_2(O_2CCPh_3)_4 \cdot Py$. Positions of chromium, oxygen, and bridging carbon atoms were located with a Patterson interpretation provided by the SHELXS-86 program package. Attempts to locate additional atoms in a difference Fourier map failed. The refinement also showed large correlations, with one Cr–O distance being very short, the other very long. Additional atoms were found with a Patterson interpretation provided by SHELXL-86, aided by positions of known atoms (Cr, O, C) and by partial structure expansion. After all the atoms in the chromium dimer were located, the refinement did not present any particular difficulties. A difference Fourier map revealed a rough outline of the axially coordinated pyridine molecule. The pyridine ring was at the angle to the Cr–Cr bond, which seemed unreasonable at first. We therefore tried to force the pyridine ring to be aligned with the Cr–Cr vector, but it could not be refined in this position. After careful examination of the packing diagram, it became apparent that the pyridine was off line because of packing constraints (see Discussion section). There is room for only one molecule of pyridine per dimer, and even then space limitations require it to be off line. Finally, the site symmetry requires that it be fourfold disordered. Once all of this was appreciated a disordered model was

(5) Calculations were done on a MicroVax II with an SDP package software and with SHELX-76 program package.

Table I. Crystallographic Data for $Cr_2(O_2CCPh_3)_4 \cdot C_6H_6$ (**1**) with Mo and Cu Radiation and $Cr_2(O_2CCPh_3)_4 \cdot Py$ (**2**) and $Cr_2(O_2CCPh_3) \cdot 2Et_2O$ (**3**)

formula	$C_{86}H_{66}O_8Cr_2$		$Cr_2C_{85}H_{65}NO_8$	$Cr_2O_{10}C_{88}H_{80}$
formula wt	1331.5		1332.4	1401.60
space group	$P/4nnc$		$I\bar{4}$	$C2/c$
systematic absences	$hk0$, $h + k = 2n + 1$ $0kl$, $k + l = 2n + 1$ hhl, $l = 2n + 1$		$h + k + l = 2n + 1$	hkl, $h + k = 2n + 1$; $00l$, $l = 2n + 1$
a, Å	20.775 (10)	20.787 (4)	18.268 (4)	21.535 (5)
b, Å	20.775 (10)	20.787 (4)	18.268 (4)	17.065 (5)
c, Å	17.710 (8)	17.710 (3)	10.919 (2)	20.498 (4)
α, deg	90.0	90.0	90.0	90.0
β, deg	90.0	90.0	90.0	90.65 (3)
γ, deg	90.0	90.0	90.0	90.0
V, Å^3	7643 (11)	7653 (3)	3644 (2)	7532 (3)
Z	4	4	2	4
d_{calcd}, g/cm^3	1.157	1.156	1.214	1.236
cryst size, mm	0.4 × 0.3 × 0.2	0.29 × 0.32 × 0.42	0.45 × 0.40 × 0.30	0.3 × 0.3 × 0.4
μ, cm^{-1}	3.273	27.799	3.437	3.370
data collcn instrmnt	P3	Nicolet $P\bar{1}$	CAD-4	AFC5R, Rigaku
radiatn (monochrmtd in incidnt beam)	Mo Kα ($\lambda_{\bar{\alpha}}$ = 0.71073 Å)	Cu Kα ($\lambda_{\bar{\alpha}}$ = 1.54184 Å)	Mo Kα ($\lambda_{\bar{\alpha}}$ = 0.71073 Å)	
orienttn reflcns, no., range (2θ)	25, 10–25	15, $2\theta > 45°$	25, 20–30	25, 30–40
temp, °C	21	20	19	21
scan method	ω–2θ	ω–2θ	ω–2θ	ω–2θ
data col. range, 2θ, deg	4–40°	3.0–105.1	$4 < 2\theta < 45$	$4 < 2\theta < 50$
no. unique data, tot. with $F_o^2 > 3\sigma(F_o^2)$	1128, 589	2276, 858	1041, 770	2969, 1878
no. of params refined	175	211	181	366
trans. factors, max, min.		1.000, 0.857	1.00, 0.99	
R[a]	0.0681	0.0640	0.0614	0.079
R_w[b]	0.0828	0.0805	0.0733	0.1092
quality-of-fit indctr[c]	1.666	1.641	1.664	1.965
largest shift/esd, final cycle	0.07	0.12	0.1	0.12
largest peak, e/Å^3	0.58	0.48	0.36	0.75

[a] $R = \sum||F_o| - |F_c||/\sum|F_o|$. [b] $R_w = [\sum w(|F_o| - |F_c|)^2/\sum w|F_o|^2]^{1/2}$; $w = 1/\sigma^2(|F_o|)$. [c] Quality-of-fit = $[\sum w(|F_o| - |F_c|)^2/(N_{obsd} - N_{params})]^{1/2}$.

devised and successfully refined. Phenyl rings were treated as perfect hexagons and so was the pyridine molecule. Hydrogen atoms were added to the phenyl rings at calculated distances with a common thermal parameter and included in the refinement. All the atoms, except for the pyridine molecule, were refined anisotropically. The final residuals were $R = 0.0614$ and $R_w = 0.0733$ for 770 reflections with $F_o^2 > 3\sigma(F_o)^2$ and 181 parameters refined. Once again, phenyl groups showed large thermal motions, thus accounting for the weakness of high-angle reflections.

Computational Procedures. The atomic coordinates used in the calculation of the electronic structure of $Cr_2(O_2CH)_4(C_6H_6)_2$ were based on the crystal structure data for the real system, $Cr_2(O_2CCPh_3)_4(C_6H_6)_2$. The $Cr_2(O_2CH)_4$ fragment was idealized to possess D_{4h} symmetry. The two benzene rings were placed in an eclipsed geometry on each side of the $Cr_2(O_2CH)_4$ unit and with their centers of gravity on the Cr–Cr axis (z axis). The whole system, therefore, belongs to the D_{2h} point group. The distance from a benzene plane to the adjacent Cr atom, taken from the crystal data, was equal to 3.299 Å. The calculation was also carried out for the system with this distance set equal to 2.3 Å. The Cr–Cr bond distance used throughout was that in the real compound, while other bond lengths and angles were slightly different. They are, in the $Cr_2(O_2CH)_4$ fragment, as follows: Cr–O, 1.982 Å; O–C, 1.280 Å; C–H, 1.08 Å; Cr–Cr–O, 90°; and O–C–O, 123.5°; for the benzene fragment, they are as follows: C–C, 1.397 Å; C–H, 1.084 Å; C–C–C, 120°; and C–C–H, 120°.

There are difficulties in performing an Xα-SW calculation on such a system which has low symmetry (D_{2h}) but contains a high symmetry fragment (D_{4h}). Some energy levels of the $Cr_2(O_2CH)_4$ fragment belonging to different symmetry species in the D_{4h} point group can belong to the same symmetry species in the D_{2h} point group. Some of these levels may be energetically very close to each other, since the energy values and compositions of most of the fragment orbitals change little from the fragments to the combined system; they may therefore be easily missed during the energy search procedure of the calculation. In addition, numerical convergence may not be easily reached in a calculation involving so many atoms.

Our calculation was actually performed in three steps, and a procedure similar to that in ref 6 was used. We first obtained a converged result for the $Cr_2(O_2CH)_4$ fragment in D_{4h} symmetry. Then a calculation on the $(C_6H_6)_2$ fragment using D_{2h} symmetry was carried out to the same level of convergence. In the second step the geometry used for $(C_6H_6)_2$ was the same as it was in $Cr_2(O_2CH)_4(C_6H_6)_2$. The converged potentials of the fragments were then used to compose a starting potential for the whole system. The calculation on the whole system was continued in D_{2h} symmetry until convergence was reached. The basis functions included all spherical harmonics through $l = 4$ on the outer sphere, $l = 2$ on Cr, $l = 1$ on O and C, and $l = 0$ on H.

The starting potentials for each fragment were superpositions of neutral atomic Herman–Skillman potentials of the constituent atoms. The α values used for each atom were taken from the compilation of Schwarz.[7] The atomic sphere radii were chosen as 88.5% of the atomic number radii[8] for $Cr_2(O_2CH)_4$ and 88% for $(C_6H_6)_2$. The same values of the atomic sphere radii were also used in the calculation of $Cr_2(O_2CH)_4(C_6H_6)_2$. The sphere radii and the α parameters are summarized in Table II.

Table II. Sphere Radii (Å) and α Parameters for $Cr_2(O_2CH)_4(C_6H_6)_2$

atom	sphere radius	α
outer sphere	5.7518	0.752 33
Cr	1.2654	0.713 52
O	0.9196	0.744 47
C	0.8487	0.759 28
H	0.6806	0.777 25
C(benzene)	0.9167	0.759 28
H(benzene)	0.6766	0.777 25

Results and Discussion

General Comments. In each of these three compounds the key building block, the $Cr_2(O_2CCPh_3)_4$ core, is essentially the same. Figures 1, 2, and 3 show these, along with the appropriate axial

(6) Bursten, B. E.; Cotton, F. A. *Inorg. Chem.* **1981**, *20*, 3042.

(7) Schwarz, K. *Phys. Rev. B* **1972**, *5*, 2466. Schwarz, K. *Theor. Chim. Acta* **1974**, *34*, 225.

(8) Norman, J. G., Jr. *Mol. Phys.* **1976**, *31*, 1191.

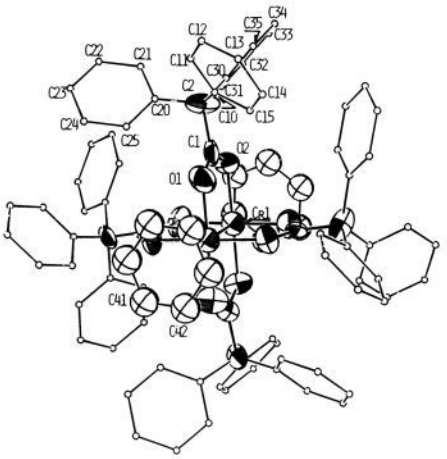

Figure 1. An ORTEP drawing of the $Cr_2(O_2CCPh_3)_4$ molecule in compound **1**, showing also two axial benzene molecules, each of which is shared with a neighboring dichromium unit. Phenyl carbon atoms are represented by arbitrarily small circles, while all other atoms are represented by their thermal displacement ellipsoids at the 50% level.

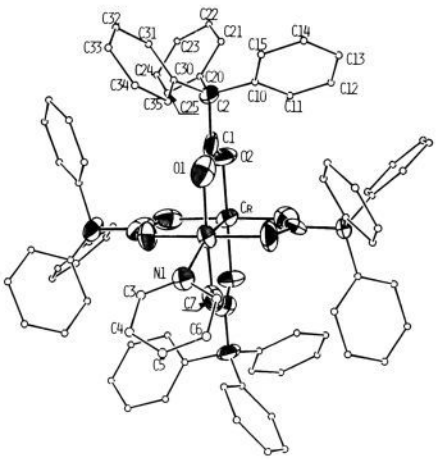

Figure 2. An ORTEP drawing of the $Cr_2(O_2CCPh_3)_4$ molecule in compound **2**, showing also one axially coordinated pyridine molecule. The phenyl and pyridine carbon atoms are represented by arbitrarily small circles, while all other atoms are represented by their thermal displacement ellipsoids at the 50% level.

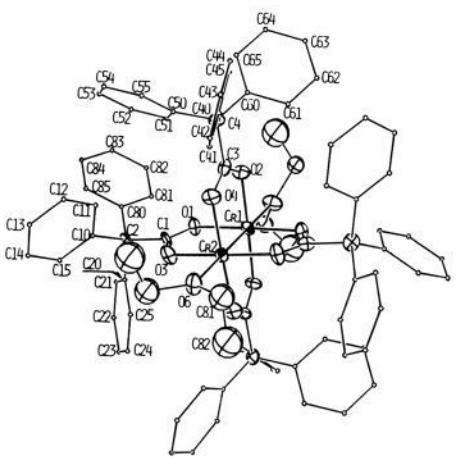

Figure 3. An ORTEP drawing of the $Cr_2(O_2CCPh_3)_4(Et_2O)_2$ molecule in compound **3**. The phenyl carbon atoms are represented by arbitrarily small circles while the others are represented by their thermal displacement ellipsoids at the 50% level.

ligands, for compounds **1**, **2**, and **3**, respectively. The arrangement of the CPh_3 groups is such as to place one phenyl group of each

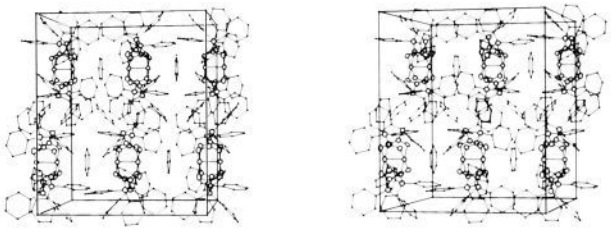

Figure 4. A stereo ORTEP drawing of the unit cell of compound **1**. The crystal axes are as follows: *a*, down; *b*, toward viewer; *c*, horizontal.

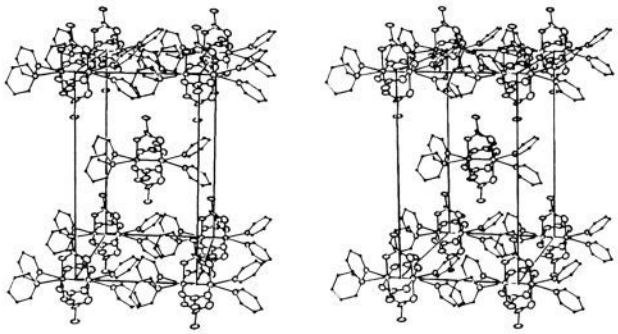

Figure 5. A stereo ORTEP drawing of the unit cell of compound **2**, with phenyl rings omitted for clarity. The axes are oriented as in Figure 4.

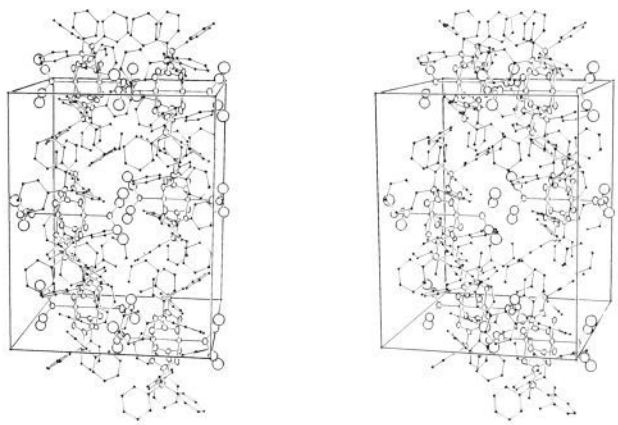

Figure 6. A stereo ORTEP drawing of the unit cell of compound **3**. The crystal axes are as follows: *a*, down; *b*, horizontal; *c*, toward viewer.

in the mid-plane (i.e., a plane that perpendicularly bisects the Cr–Cr axis) of the molecule, all in the same cyclic sense about the Cr–Cr axis. Each of these mid-plane phenyl groups is tucked into the cleft between the non-mid-plane phenyl groups of a neighboring CPh_3 group. The entire arrangement achieves an optimal intramolecular packing which is relatively rigid. It directs eight of the 12 phenyl groups out beside, and beyond, the eight oxygen atoms, and thus makes it impossible for these molecules to adopt the infinite kinked chain arrangement found in so many other $M_2(O_2CR)_4$ compounds, where each molecule uses two of its oxygen atoms to form axial bonds to its neighbors.

Tables III–V give the positional parameters and isotropic (or equivalent isotropic) thermal displacement parameters for the three compounds, while Tables VI–VIII give the important bond distances and angles. The major dimensions of these $Cr_2(O_2CCPh_3)_4$ units are similar to those in the many other tetracarboxylatodichromium compounds that have been structurally characterized.[1,9]

The three compounds display different forms of packing, which shows that this is not controlled solely by the intermolecular contacts between peripheral phenyl groups. However, there is one feature common to the packing of all three compounds, as can be seen by inspection of Figures 4–6. In each case, there are infinite linear arrays with colinear Cr–Cr axes. The differences

(9) Cotton, F. A.; Wang, W. *Nouv. J. Chim.* **1984**, *8*, 331.

Table III. Positional and Isotropic Equivalent Displacement Parameters and Their Estimated Standard Deviations

atom	*x*	*y*	*z*	*B* (Å²)	atom	*x*	*y*	*z*	*B* (Å²)
				$Cr_2(O_2CCPh_3)_4 \cdot C_6H_6$					
Cr(1)	0.2500	0.7500	0.0637 (2)	4.45 (6)	C(23)	0.3022 (8)	0.438 (1)	0.0624 (9)	13 (1)
O(1)	0.3241 (7)	0.6920 (8)	0.067 (1)	6.1 (6)	C(24)	0.2892 (8)	0.493 (1)	0.1037 (9)	10 (1)
O(2)	0.1888 (6)	0.6752 (7)	0.0607 (7)	4.6 (4)	C(25)	0.3198 (8)	0.551 (1)	0.0850 (9)	7.7 (9)
C(1)	0.3462 (9)	0.6711 (9)	0.007 (2)	4.4 (6)	C(20)	0.3634 (8)	0.553 (1)	0.0251 (9)	7.1 (9)
C(2)	0.3990 (8)	0.6167 (9)	0.004 (2)	5.9 (6)	C(31)	0.3949 (7)	0.6003 (8)	−0.139 (2)	9.4 (9)
C(11)	0.477 (1)	0.5841 (8)	0.103 (1)	7.2 (8)	C(32)	0.4253 (7)	0.5966 (8)	−0.209 (2)	12 (1)
C(12)	0.524 (1)	0.5956 (8)	0.156 (1)	10 (1)	C(33)	0.4918 (7)	0.6046 (8)	−0.214 (2)	11 (1)
C(13)	0.542 (1)	0.6586 (8)	0.174 (1)	8.9 (9)	C(34)	0.5280 (7)	0.6162 (8)	−0.149 (2)	10 (1)
C(14)	0.512 (1)	0.7101 (8)	0.137 (1)	8.2 (9)	C(35)	0.4976 (7)	0.6198 (8)	−0.079 (2)	7.3 (8)
C(15)	0.464 (1)	0.6986 (8)	0.084 (1)	7.9 (9)	C(30)	0.4311 (7)	0.6119 (8)	−0.074 (2)	5.8 (8)
C(10)	0.446 (1)	0.6356 (8)	0.067 (1)	6.0 (8)	C(41)	0.319 (2)	0.7500	0.2500	12 (1)[a]
C(21)	0.3763 (8)	0.497 (1)	−0.0162 (9)	8.8 (9)	C(42)	0.284 (1)	0.694 (1)	0.251 (2)	12.7 (8)[a]
C(22)	0.3457 (8)	0.440 (1)	0.0025 (9)	14 (1)					
				$Cr_2(O_2CCPh_3)_4 \cdot C_6H_6$ ⟨Cu Radiation⟩					
Cr(1)	0.2500	0.7500	0.0638 (1)	5.23 (9)	C(23)	0.304 (1)	0.437 (1)	0.061 (2)	15 (1)
O(1)	0.3236 (4)	0.6914 (4)	0.0655 (6)	6.5 (3)	C(24)	0.2899 (8)	0.493 (1)	0.104 (1)	11.1 (7)
O(2)	0.1894 (4)	0.6750 (4)	0.0599 (5)	5.8 (3)	C(25)	0.3211 (8)	0.5512 (7)	0.084 (1)	8.6 (5)
C(1)	0.3465 (5)	0.6701 (6)	0.004 (1)	6.0 (3)	C(20)	0.3628 (7)	0.5545 (8)	0.0244 (9)	7.7 (5)
C(2)	0.3991 (6)	0.6175 (6)	0.006 (1)	6.3 (3)	C(31)	0.3964 (9)	0.6002 (7)	−0.137 (1)	9.7 (5)
C(11)	0.4779 (8)	0.5832 (8)	0.1023 (9)	8.0 (5)	C(32)	0.425 (1)	0.5983 (9)	−0.2076 (9)	13.3 (8)
C(12)	0.525 (1)	0.597 (1)	0.156 (1)	10.6 (7)	C(33)	0.491 (1)	0.604 (1)	−0.215 (1)	13.2 (8)
C(13)	0.5425 (9)	0.657 (1)	0.1729 (9)	10.5 (6)	C(34)	0.527 (1)	0.6143 (8)	−0.152 (1)	11.3 (6)
C(14)	0.5120 (8)	0.7098 (8)	0.138 (1)	9.5 (6)	C(35)	0.4964 (9)	0.6196 (7)	−0.0790 (9)	8.2 (5)
C(15)	0.4646 (7)	0.6956 (8)	0.082 (1)	8.6 (5)	C(30)	0.4311 (8)	0.6128 (7)	−0.072 (1)	7.9 (5)
C(10)	0.4469 (7)	0.6338 (9)	0.0658 (9)	7.0 (5)	C(41)	0.320 (2)	0.7500	0.2500	15.2 (9)[a]
C(21)	0.3769 (8)	0.4969 (8)	−0.017 (1)	10.2 (6)	C(42)	0.2843 (7)	0.6953 (8)	0.250 (1)	14.1 (6)[a]
C(22)	0.344 (1)	0.438 (1)	0.000 (2)	14.4 (9)					

[a] Atoms were refined isotropically. Anisotropically refined atoms are given in the form of the equivalent isotropic displacement parameter defined as the following: $(^4/_3)[a^2\beta_{11} + b^2\beta_{22} + c^2\beta_{33} + ab(\cos\gamma)\beta_{12} + ac(\cos\beta)\beta_{13} + bc(\cos\alpha)\beta_{23}]$.

Table IV. Positional and Isotropic Equivalent Displacement Parameters and Their Estimated Standard Deviations for $Cr_2(O_2CCPh_3)_4 \cdot Py$

atom	*x*	*y*	*z*	*B* (Å²)	atom	*x*	*y*	*z*	*B* (Å²)
Cr	0.0000	0.0000	−0.1091 (3)	3.75 (9)	C15	0.1730 (6)	−0.2694 (5)	−0.062 (1)	7.2 (6)
O1	0.0238 (6)	−0.1071 (7)	−0.100 (1)	6.0 (4)	C10	0.1351 (6)	−0.2236 (5)	0.018 (1)	5.6 (4)
O2	−0.1071 (5)	−0.0241 (6)	−0.102 (1)	5.1 (3)	C21	0.0597 (5)	−0.2953 (7)	0.216 (1)	8.0 (6)
C1	0.0301 (6)	−0.1386 (7)	0.005 (3)	6.1 (5)	C22	0.0273 (5)	−0.3263 (7)	0.319 (1)	10.3 (8)
C2	0.0497 (6)	−0.2223 (6)	0.020 (2)	5.1 (5)	C23	−0.0461 (5)	−0.3122 (7)	0.346 (1)	9.9 (8)
C3	0.041 (2)	0.089 (1)	0.360 (3)	12 (3)[a]	C24	−0.0870 (5)	−0.2670 (7)	0.269 (1)	8.1 (6)
C4	0.082 (2)	0.101 (1)	0.466 (3)	4 (1)[a]	C25	−0.0546 (5)	−0.2359 (7)	0.165 (1)	7.1 (6)
C5	0.120 (2)	0.043 (1)	0.520 (3)	6 (1)[a]	C20	0.0188 (5)	−0.2501 (7)	0.139 (1)	6.1 (6)
C6	0.116 (2)	−0.027 (1)	0.469 (3)	5 (1)[a]	C31	−0.0123 (6)	−0.3356 (6)	−0.070 (1)	8.8 (7)
C7	0.075 (2)	−0.039 (1)	0.364 (3)	5 (1)[a]	C32	−0.0386 (6)	−0.3795 (6)	−0.165 (1)	9.0 (8)
N1	0.037 (2)	0.019 (1)	0.309 (3)	3.5 (9)[a]	C33	−0.0337 (6)	−0.3554 (6)	−0.286 (1)	11 (1)
C11	0.1735 (6)	−0.1808 (5)	0.103 (1)	7.2 (5)	C34	−0.0026 (6)	−0.2874 (6)	−0.312 (1)	10.6 (9)
C12	0.2498 (6)	−0.1838 (5)	0.106 (1)	7.8 (5)	C35	0.0236 (6)	−0.2435 (6)	−0.217 (1)	9.2 (8)
C13	0.2876 (6)	−0.2297 (5)	0.026 (1)	8.8 (7)	C30	0.0188 (6)	−0.2676 (6)	0.096 (1)	6.8 (5)
C14	0.2492 (6)	−0.2725 (5)	−0.058 (1)	9.0 (7)					

[a] Atoms were refined isotropically. Anisotropically refined atoms are given in the form of the equivalent isotropic displacement parameter defined as follows: $(^4/_3)[a^2\beta_{11} + b^2\beta_{22} + c^2\beta_{33} + ab(\cos\gamma)\beta_{12} + ac(\cos\beta)\beta_{13} + bc(\cos\alpha)\beta_{23}]$.

are in (1) the relationship of adjacent linear arrays (the relative register) and (2) the intermolecular Cr···Cr distances. In the case of compound **1** (Figure 4) the chains are in register. This means that there are sheets of $Cr_2(O_2CCPh_3)_4$ molecules alternating with sheets of coplanar benzene rings. The intermolecular Cr···Cr distances are 6.590 Å.

For the pyridine adduct, compound **2**, the packing is shown in Figure 5, where the phenyl groups have been omitted for clarity and the four quarter molecules of pyridine belonging to each dichromium unit are shown in full. The Supplementary Material includes an alternative drawing in which all phenyl groups are shown, but only the nitrogen atoms of the pyridine molecules are shown. It is clear that the main qualitative difference in the packing here as compared to that in compound **1** is that half the linear arrays are one half a repeat distance out of register with the other half. The intermolecular Cr···Cr distances are 8.40 Å, i.e., larger than for **1**. This is determined mainly by interchain packing.

Turning now to the packing in compound **3**, we see in Figure 6 that again half the linear arrays are out of register with the other half by one half the repeat distance. Here the intermolecular Cr···Cr distance is very long, viz., 14.77 Å, thus allowing room for two diethyl ether molecules in each cavity.

Compound 1. This is the most remarkable of the three compounds. The packing of the $Cr_2(O_2CCPh_3)_4$ molecules is such as to provide cavities that are short and wide into which benzene molecules can fit. The Cr–Cr distance is shortest one yet seen in a crystalline $Cr_2(O_2CR)_4$ or $Cr_2(O_2CR)_4L_{1\text{ or }2}$ compound. On the other hand, it is far longer than the Cr–Cr distance in the isolated (i.e., gaseous) $Cr_2(O_2CCH_3)_4$ molecule,[10] 1.97 Å. These facts suggested to us that the benzene molecules are engaged in some type of axial bonding to the Cr_2 units that is strong enough to weaken and lengthen the Cr–Cr bond.

From a qualitative point of view, this sort of interaction has some precedent, although no really close parallel exists, to our knowledge. There are, of course, complexes of Ag^+ and Tl^+ ions with benzene and other aromatic compounds, but these differ in that the metal atom lies well off center. The principal acceptor orbital of the metal atom is its valence shell *s* orbital, and for this

(10) Ketkar, S. N.; Fink, M. *J. Am. Chem. Soc.* **1985**, *107*, 338.

Table V. Positional and Isotropic Equivalent Displacement Parameters and Their Estimated Standard Deviations for $Cr_2(O_2CCPh_3)_4 \cdot 2Et_2O$

atom	x	y	z	B (Å²)	atom	x	y	z	B (Å²)
Cr(1)	0.0000	0.3140 (2)	0.2500	3.66 (9)	C(25)	0.0723 (4)	0.1909 (5)	0.4617 (5)	5.5 (4)
Cr(2)	0.0000	0.1790 (2)	0.2500	3.57 (9)	C(20)	0.1164 (4)	0.2483 (5)	0.4481 (5)	4.2 (3)
O(1)	0.0728 (4)	0.3102 (5)	0.3113 (4)	4.2 (3)	C(31)	0.1689 (4)	0.3929 (7)	0.3620 (4)	4.7 (4)
O(2)	−0.0559 (4)	0.3106 (6)	0.3266 (4)	4.3 (3)	C(32)	0.2094 (4)	0.4565 (7)	0.3578 (4)	6.4 (5)
O(3)	0.0693 (5)	0.1820 (6)	0.3148 (5)	5.2 (3)	C(33)	0.2730 (4)	0.4456 (7)	0.3676 (4)	5.9 (5)
O(4)	−0.0614 (5)	0.1823 (6)	0.3216 (5)	5.2 (3)	C(34)	0.2962 (4)	0.3711 (7)	0.3815 (4)	5.5 (4)
C(1)	0.0931 (6)	0.246 (1)	0.3299 (5)	4.0 (3)	C(35)	0.2558 (4)	0.3075 (7)	0.3857 (4)	5.5 (4)
C(2)	0.1475 (6)	0.2482 (9)	0.3821 (6)	4.2 (3)	C(30)	0.1921 (4)	0.3184 (7)	0.3759 (4)	3.8 (4)
C(3)	−0.0748 (5)	0.245 (1)	0.3473 (6)	3.9 (3)	C(41)	−0.0945 (5)	0.1028 (7)	0.4305 (4)	7.0 (5)
C(4)	−0.1237 (5)	0.2460 (9)	0.4054 (6)	4.1 (3)	C(42)	−0.0924 (5)	0.0394 (7)	0.4734 (4)	8.4 (6)
O(5)	0.0000	0.4486 (8)	0.2500	6.4 (5)	C(43)	−0.1127 (5)	0.0482 (7)	0.5373 (4)	6.9 (6)
C(71A)	−0.005 (2)	0.492 (2)	0.316 (2)	6.4 (8)[a]	C(44)	−0.1352 (5)	0.1204 (7)	0.5584 (4)	9.9 (7)
C(71B)	−0.056 (2)	0.500 (3)	0.278 (2)	11 (1)[a]	C(45)	−0.1374 (5)	0.1839 (7)	0.5155 (4)	8.1 (6)
C(72)	−0.063 (2)	0.512 (2)	0.331 (2)	17 (1)[a]	C(40)	−0.1171 (5)	0.1751 (7)	0.4515 (4)	5.0 (5)
O(6)	0.0000	0.0439 (8)	0.2500	6.3 (5)	C(51)	−0.1989 (5)	0.3064 (5)	0.3224 (5)	5.2 (4)
C(81)	0.048 (1)	−0.001 (1)	0.289 (1)	12.0 (7)[a]	C(52)	−0.2566 (5)	0.3104 (5)	0.2909 (5)	6.1 (5)
C(82)	0.093 (1)	−0.026 (2)	0.246 (1)	17 (1)[a]	C(53)	−0.3025 (5)	0.2554 (5)	0.3050 (5)	7.8 (6)
C(11)	0.2031 (5)	0.1483 (7)	0.3096 (5)	6.5 (5)	C(54)	−0.2907 (5)	0.1965 (5)	0.3507 (5)	7.8 (6)
C(12)	0.2394 (5)	0.0816 (7)	0.3005 (5)	8.4 (6)	C(55)	−0.2330 (5)	0.1925 (5)	0.3822 (5)	5.8 (4)
C(13)	0.2585 (5)	0.0371 (7)	0.3542 (5)	10.3 (8)	C(50)	−0.1871 (5)	0.2474 (5)	0.3681 (5)	4.5 (3)
C(14)	0.2413 (5)	0.0593 (7)	0.4169 (5)	10.1 (8)	C(61)	−0.0544 (4)	0.3404 (6)	0.4642 (5)	5.0 (4)
C(15)	0.2050 (5)	0.1260 (7)	0.4260 (5)	6.5 (5)	C(62)	−0.0448 (4)	0.4048 (6)	0.5050 (5)	6.5 (5)
C(10)	0.1859 (5)	0.1705 (7)	0.3723 (5)	4.9 (5)	C(63)	−0.0953 (4)	0.4491 (6)	0.5260 (5)	7.9 (6)
C(21)	0.1330 (4)	0.3030 (5)	0.4957 (5)	5.7 (4)	C(64)	−0.1554 (4)	0.4289 (6)	0.5061 (5)	6.3 (5)
C(22)	0.1055 (4)	0.3002 (5)	0.5570 (5)	7.7 (6)	C(65)	−0.1650 (4)	0.3645 (6)	0.4653 (5)	5.2 (4)
C(23)	0.0615 (4)	0.2428 (5)	0.5706 (5)	7.7 (6)	C(60)	−0.1145 (4)	0.3203 (6)	0.4444 (5)	3.6 (4)
C(24)	0.0449 (4)	0.1881 (5)	0.5229 (5)	6.8 (5)					

[a] Atoms were refined isotropically. Anisotropically refined atoms are given in the form of the equivalent isotropic displacement parameter defined as follows: $(^4/_3)[a^2\beta_{11} + b^2\beta_{22} + c^2\beta_{33} + ab(\cos\gamma)\beta_{12} + ac(\cos\beta)\beta_{13} + bc(\cos\alpha)\beta_{23}]$.

Table VI. Selected Bond Distances (Å) and Angles (deg)[a]

$Cr_2(O_2CCPh_3)_4 \cdot C_6H_6$

atom 1	atom 2	distance	atom 1	atom 2	distance	atom 1	atom 2	distance
Cr(1)	Cr(1)	2.256 (4)	O(1)	C(1)	1.23 (4)	C(2)	C(10)	1.54 (3)
Cr(1)	O(1)	1.956 (15)	O(2)	C(1)	1.33 (4)	C(2)	C(20)	1.57 (3)
Cr(1)	O(2)	2.008 (13)	C(1)	C(2)	1.58 (3)	C(2)	C(30)	1.52 (4)

atom 1	atom 2	atom 3	angle	atom 1	atom 2	atom 3	angle	atom 1	atom 2	atom 3	angle
Cr(1)	Cr(1)	O(1)	91.5 (5)	Cr(1)	O(1)	C(1)	119 (2)	C(1)	C(2)	C(20)	106 (2)
Cr(1)	Cr(1)	O(2)	88.5 (4)	Cr(1)	O(2)	C(1)	117 (1)	C(1)	C(2)	C(30)	113 (2)
O(1)	Cr(1)	O(1)	176.9 (7)	O(1)	C(1)	O(2)	123 (2)	C(10)	C(2)	C(20)	110 (2)
O(1)	Cr(1)	O(2)	91.3 (6)	O(1)	C(1)	C(2)	123 (3)	C(10)	C(2)	C(30)	113 (2)
O(1)	Cr(1)	O(2)	88.8 (6)	O(2)	C(1)	C(2)	113 (2)	C(20)	C(2)	C(30)	112 (2)
O(2)	Cr(1)	O(2)	176.9 (6)	C(1)	C(2)	C(10)	104 (2)				

$Cr_2(O_2CCPh_3)_4 \cdot C_6H_6$ (Cu Radiation)

atom 1	atom 2	distance	atom 1	atom 2	distance	atom 1	atom 2	distance
Cr(1)	Cr(1)	2.261 (3)	Cr(1)	O(1)	1.956 (9)	Cr(1)	O(2)	2.005 (8)
O(1)	C(1)	1.26 (2)	O(2)	C(1)	1.29 (2)	C(1)	C(2)	1.55 (2)
C(2)	C(10)	1.49 (2)	C(2)	C(20)	1.55 (2)	C(2)	C(30)	1.53 (2)
C(41)	C(42)	1.35 (2)	C(42)	C(42)	1.43 (2)			

atom 1	atom 2	atom 3	angle	atom 1	atom 2	atom 3	angle	atom 1	atom 2	atom 3	angle
Cr(1)	Cr(1)	O(1)	90.8 (3)	Cr(1)	Cr(1)	O(2)	88.0 (3)	O(1)	Cr(1)	O(1)	178.3 (4)
O(1)	Cr(1)	O(2)	90.5 (3)	O(1)	Cr(1)	O(2)	89.6 (3)	O(2)	Cr(1)	O(2)	176.0 (4)
Cr(1)	O(1)	C(1)	120.0 (9)	Cr(1)	O(2)	C(1)	119.8 (8)	O(1)	C(1)	O(2)	121 (1)
O(1)	C(1)	C(2)	120 (2)	O(2)	C(1)	C(2)	119 (2)	C(42)	C(41)	C(42)	114 (2)
C(41)	C(42)	C(42)	123 (2)								

[a] Numbers in parentheses are estimated standard deviations in the least significant digits.

Table VII. Selected Bond Distances (Å) and Angles (deg) for $Cr_2(O_2CCPh_3)_4 \cdot Py$[a]

atom 1	atom 2	distance	atom 1	atom 2	distance	atom 1	atom 2	distance
Cr	Cr	2.383 (4)	Cr	N1	2.31 (4)	O2	C1	1.22 (3)
Cr	O1	2.007 (12)	O1	C1	1.28 (3)	C1	C2	1.58 (2)
Cr	O2	2.007 (9)						

atom 1	atom 2	atom 3	angle	atom 1	atom 2	atom 3	angle	atom 1	atom 2	atom 3	angle
Cr	Cr	O1	87.1 (5)	O1	Cr	O2	90.0 (4)	O2	Cr	N1	87.3 (8)
Cr	Cr	O2	87.8 (4)	O1	Cr	N1	74 (1)	Cr	O1	C1	120 (1)
Cr	Cr	N1	160.7 (8)	O1	Cr	N1	112 (1)	Cr	O2	C1	121 (1)
O1	Cr	O1	174.1 (7)	O2	Cr	O2	175.7 (6)	O1	C1	O2	124 (1)
O1	Cr	O2	89.7 (4)	O2	Cr	N1	96.8 (8)				

[a] Numbers in parentheses are estimated standard deviations in the least significant digits.

Table VIII. Selected Bond Distances (Å) and Angles (deg) for $Cr_2(O_2CCPh_3)_4 \cdot (Et_2O)_2$[a]

atom 1	atom 2	distance	atom 1	atom 2	distance	atom 1	atom 2	distance
Cr(1)	Cr(2)	2.303 (4)	Cr(2)	O(4)	1.987 (10)	O(4)	C(3)	1.22 (2)
Cr(1)	O(1)	1.999 (9)	Cr(2)	O(6)	2.305 (14)	C(1)	C(2)	1.58 (2)
Cr(1)	O(2)	1.990 (9)	O(1)	C(1)	1.23 (2)	C(3)	C(4)	1.60 (2)
Cr(1)	O(5)	2.298 (14)	O(2)	C(3)	1.27 (2)			
Cr(2)	O(3)	1.988 (10)	O(3)	C(1)	1.25 (2)			

atom 1	atom 2	atom 3	angle	atom 1	atom 2	atom 3	angle	atom 1	atom 2	atom 3	angle
Cr(2)	Cr(1)	O(1)	88.2 (3)	O(1)	Cr(1)	O(5)	91.8 (3)	O(3)	Cr(2)	O(3)	177.0 (4)
Cr(2)	Cr(1)	O(2)	88.3 (3)	O(2)	Cr(1)	O(2)	176.7 (4)	O(3)	Cr(2)	O(4)	90.4 (4)
Cr(2)	Cr(1)	O(5)	180.00 (0)	O(2)	Cr(1)	O(5)	91.7 (3)	O(3)	Cr(2)	O(4)	89.6 (4)
O(1)	Cr(1)	O(1)	176.4 (4)	Cr(1)	Cr(2)	O(3)	88.5 (3)	O(3)	Cr(2)	O(6)	91.5 (3)
O(1)	Cr(1)	O(2)	88.9 (4)	Cr(1)	Cr(2)	O(4)	88.4 (3)	O(4)	Cr(2)	O(4)	176.7 (4)
O(1)	Cr(1)	O(2)	91.0 (4)	Cr(1)	Cr(2)	O(6)	180.00 (0)	O(4)	Cr(2)	O(6)	91.6 (3)

[a] Numbers in parentheses are estimated standard deviations in the least significant digits.

to receive electron density from the HOMO of the benzene molecule which has a node bisecting the ring, the metal atom must lie to one side.

Structurally closer to the present situation are the crystalline benzene adducts of Cl_2 and Br_2, in which there are infinite chains of alternating benzene molecules and X_2 molecules.[11] These interactions are weak (with X to ring centroid distances of 3.28 and 3.36 Å for Cl_2 and Br_2, respectively), but there is enough donation of electron density from the benzene a_{2u} orbital into the σ^* orbital of the halogen molecules to justify the term charge-transfer complex. Quite recently a hexaethylbenzene complex with $AsBr_3$, wherein two $AsBr_3$ molecules lie on opposite sides of the ring (3.16 Å, As-ring center) and interact in some as yet undefined way with it, has been reported.[12]

There are of course numerous arene–metal compounds, including the triple-decker species, $CpV(C_6H_6)VCp$[13] and $(C_6H_3Me_3)Cr(C_6H_3Me_3)Cr(C_6H_3Me_3)$,[14] with bridging benzene or mesitylene rings, but here the metal–ring interactions are very strong, with metal-to-ring centroid distances of <1.8 Å.

Since no straightforward precedent could be found for the type or magnitude of interaction we had inferred for compound **1** from its structure, we undertook some quantum mechanical calculations to see if they would give a more definite picture of the benzene–Cr_2–benzene interactions. The procedure used in the calculations (by the SW-Xα method[15]) has been summarized in the experimental section. These calculations were made for the model system (C_6H_6)-$Cr_2(O_2CH)_4$-C_6H_6 with eclipsed benzene rings and overall D_{2h} symmetry as well as for the fragments $(C_6H_6)_2$ and $Cr_2(O_2CH)_4$. For reasons explained below, the calculations of the full system were done not only at the actual chromium-ring distance of 3.299 Å but also at a shorter distance.

For the Cr–C_6H_6 distance equal to 3.299 Å, the correlation of the molecular orbitals of $Cr_2(O_2CH)_4(C_6H_6)_2$ with those of its component fragments is shown in Figure 7. For simplicity, only two groups of orbitals are involved in Figure 7. One group includes the orbitals which manifest the interaction of $Cr_2(O_2CH)_4$ with the axial benzene ligands, while the other contains the unperturbed Cr–Cr bonding and antibonding orbitals which are simply transferred from the $Cr_2(O_2CH)_4$ fragment. Some upper valence levels of $Cr_2(O_2CH)_4(C_6H_6)_2$, from the $13a_g$ orbital at the bottom to the $12b_{1u}$ orbital at the top, are listed in Table IX. The LUMO is the $5a_u$ (Cr–Cr δ^*) orbital. The HOMO is actually a degenerate level with four electrons occupying the $8b_{2g}$ and $8b_{3g}$ orbitals. Also summarized in Table IX are the energies, the percentage charge contributions, and the Cr angular contributions for these orbitals. All other levels of $Cr_2(O_2CH)_4(C_6H_6)_2$ below the $13a_g$ orbital which are not explicitly discussed here can be clearly and easily classified according to their symmetries and compositions. These low-lying levels have one-to-one correspondence with those of the component fragments.

The calculated energy level diagram for the $Cr_2(O_2CH)_4$ fragment, which is closely similar to that previously obtained by

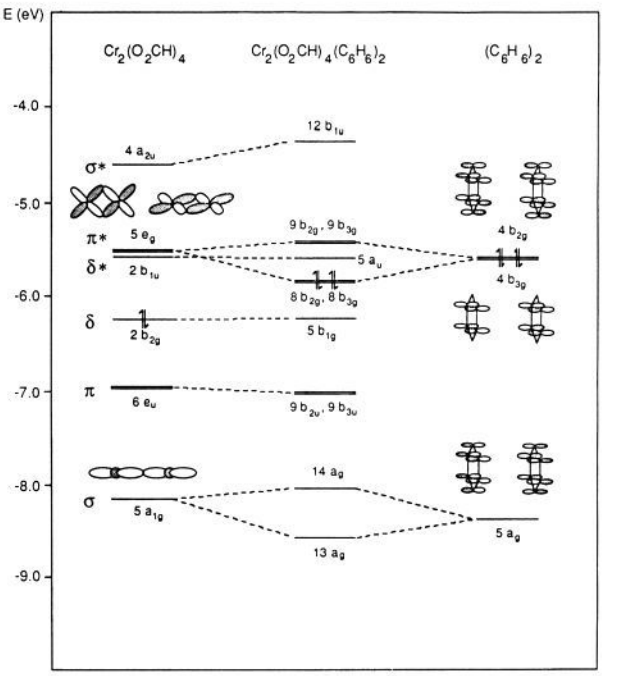

Figure 7. Molecular orbital diagram of the correlation of the orbitals of $Cr_2(O_2CH)_4(C_6H_6)_2$ to those of $Cr_2(O_2CH)_4$ and $(C_6H_6)_2$. Arrows indicate the highest occupied orbital.

Table IX. Upper Valence Molecular Orbitals of $Cr_2(O_2CH)_4(C_6H_6)_2$ at Cr–C_6H_6 Distance Equal to 3.299 Å[a]

D_{2h} level	E (eV)	% charge 2Cr	% charge $4(O_2CH)$	% charge $2(C_6H_6)$	Cr anglr contrbtn		
$12b_{1u}$	−4.35	93	6	1	1%s	3%p	96%d_{z^2}
$9b_{3g}$	−5.46	87	1	12			100%d_{yz}
$9b_{2g}$	−5.46	87	1	12			100%d_{xz}
$5a_u$	−5.59	89	11	0			100%d_{xy}
$8b_{2g}$	−5.83	20	1	79			100%d_{xz}
$8b_{3g}$	−5.83	20	1	79			100%d_{yz}
$10b_{2u}$	−5.89	2	0	98			
$10b_{3u}$	−5.89	2	0	98			
$5b_{1g}$	−6.23	93	7	0			100%d_{xy}
$9b_{3u}$	−7.04	94	6	0			100%d_{xz}
$9b_{2u}$	−7.04	94	6	0			100%d_{yz}
$14a_g$	−8.05	55	1	44	12%s	5%p	83%d_{z^2}
$11b_{1u}$	−8.40	1	1	98			
$13a_g$	−8.58	58	1	41	14%s	3%p	83%d_{z^2}

[a] The $5a_u$ orbital is the lowest unoccupied orbital.

(11) Hassel, O.; Stromme, K. O. *Acta Chem. Scand.* **1985**, *12*, 1146; **1959**, *13*, 1781.
(12) Schmidbaur, H.; Bublak, W.; Huber, B.; Müller, G. *Angew. Chem., Int. Ed. Engl.* **1987**, *26*, 234.
(13) Duff, A. W.; Jonas, K.; Goddard, R.; Kraus, H.-J.; Krüger, C. *J. Am. Chem. Soc.* **1983**, *105*, 5479.
(14) Lamanna, W. M. *J. Am. Chem. Soc.* **1986**, *108*, 2096.
(15) (a) Slater, J. C. *Quantum Theory of Molecules and Solid*; McGraw-Hill: New York, 1974; Vol. IV. (b) Johnson, K. H. *Adv. Quantum Chem.* **1973**, *7*, 143.

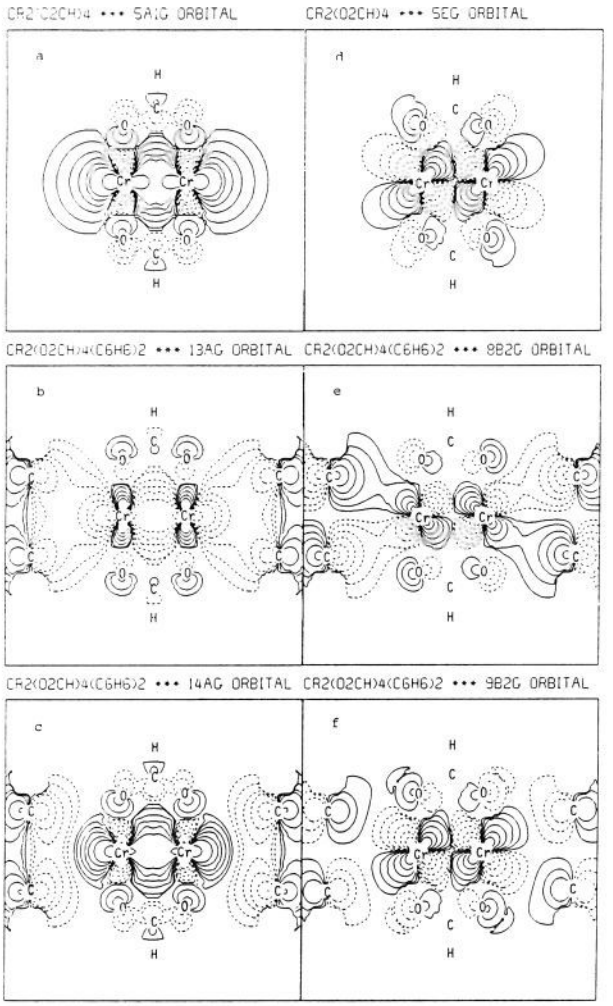

Figure 8. Contour plots of the $5a_{1g}$ and $5e_g$ orbitals of $Cr_2(O_2CH)_4$ and the $13a_g$, $14a_g$, $8b_{2g}$, and $9b_{2g}$ orbitals of $Cr_2(O_2CH)_4(C_6H_6)_2$ at the Cr–C_6H_6 distance equal to 3.299 Å. The solid and broken contour lines represent the positive and negative regions of the wave functions.

Cotton and Stanley,[16] is shown in the first column of Figure 7. The levels listed have predominantly Cr–Cr bonding or antibonding character. They are essentially combinations of the 3d orbitals of the chromium atoms, and all of them have more than 90% metal character.

It is well-known that the D_{6h} benzene molecule has as its ground-state π-electron configuration $(1a_{2u})^2(1e_{1g})^4$. For the $(C_6H_6)_2$ fragment using D_{2h} symmetry, the $1a_{2u}$ levels now combine to give effectively degenerate $5a_g$ and $5b_{1u}$ orbitals. Similarly, the pair of double-degenerate $1e_{1g}$ levels gives rise to the four $4b_{2g}$, $4b_{3g}$, $4b_{2u}$, and $4b_{3u}$ orbitals. These levels are shown in the last column of Figure 7 but only the $5a_g$, $4b_{2g}$, and $4b_{3b}$ orbitals are labeled because of their important role in interacting with the orbitals of $Cr_2(O_2CH)_4$. Schematic representations of these orbitals are also drawn in the figure. These levels have been shifted downward by 2.2 eV in obtaining the correlation diagram.

It can be seen clearly from Figure 7 and Table IX that the $5a_g$ orbital of $(C_6H_6)_2$ interacts most strongly with the $5a_{1g}$ orbital (Figure 8a) of $Cr_2(O_2CH)_4$, since the orbitals are both energetically and spatially well matched. The interaction gives rise to the $13a_g$ and $14a_g$ orbitals in $Cr_2(O_2CH)_4(C_6H_6)_2$, both of which have charge contributions derived about equally from the metal and from $(C_6H_6)_2$. As illustrated in Figure 8 (parts b and c), these two orbitals are Cr–C_6H_6 bonding and antibonding, respectively, and both have Cr–Cr σ bonding character. The orbitals are both occupied. Since there are no more occupied benzene orbitals which can interact with the $4a_{2u}$ (σ^*) orbital of $Cr_2(O_2CH)_4$, it is expected that the benzene molecules have no major effect on the Cr–Cr σ bond.

(16) Cotton, F. A.; Stanley, G. G. *Inorg. Chem.* **1977**, *16*, 2668.

Table X. Upper Valence Molecular Orbitals of $Cr_2(O_2CH)_4(C_6H_6)_2$ at Cr–C_6H_6 Distances Equal to 2.3 Å

D_{2h} level	E (eV)	% charge 2Cr	% charge $4(O_2CH)$	% charge $2(C_6H_6)$	Cr anglr contrbtn		
$12b_{1u}$	−3.66	91	6	3		2%p	98%d_{z^2}
$9b_{3g}$	−4.76	82	0	18			100%d_{yz}
$9b_{2g}$	−4.77	82	0	18			100%d_{xz}
$5a_u$	−5.30	90	10	0			100%d_{xy}
$10b_{3u}$	−5.68	33	2	65			100%d_{xz}
$10b_{2u}$	−5.68	33	3	64			100%d_{yz}
$5b_{1g}$	−5.99	92	8	0			100%d_{xy}
$8b_{2g}$	−6.25	26	7	67			100%d_{xz}
$8b_{3g}$	−6.29	26	6	68			100%d_{yz}
$9b_{3u}$	−7.06	74	6	20			100%d_{xz}
$9b_{2u}$	−7.08	74	5	21			100%d_{yz}
$14a_g$	−7.48	79	3	18	11%s	8%p	81%d_{z^2}
$11b_{1u}$	−8.86	3	15	82			
$13a_g$	−9.29	32	2	66	14%s		86%d_{z^2}

The degenerate $4b_{2g}$ and $4b_{3g}$ orbitals of $(C_6H_6)_2$ interact strongly with the empty $5e_g$ (π^*) orbital (Figure 8d) of $Cr_2(O_2CH)_4$. The interaction generates two pairs of degenerate orbitals in $Cr_2(O_2CH)_4(C_6H_6)_2$, the $8b_{2g}$ and $8b_{3g}$ orbitals which are Cr–C_6H_6 bonding and occupied, and the $9b_{2g}$ and $9b_{3g}$ orbitals which are Cr–C_6H_6 antibonding and unoccupied. It is expected that these orbitals have also Cr–Cr antibonding character. As a matter of fact, this is exactly the case as shown by the contour plots of the $8b_{2g}$ (Figure 8e) and $9b_{2g}$ (Figure 8f) orbitals. Through the occupation of the $8b_{2g}$ and $8b_{3g}$ orbitals, the fragments $Cr_2(O_2CH)_4$ and $(C_6H_6)_2$ are bonded together by donation of electrons from the axial benzene π orbitals into the formally empty π^* orbital of $Cr_2(O_2CH)_4$. The Cr–Cr π bond is thus weakened, and the bond distance should become longer than it would be without the axial ligands.

It is also noted that the $8b_{2g}$ and $8b_{3g}$ orbitals have a comparatively small amount of metal character (20%), whereas the $9b_{2g}$ and $9b_{3g}$ orbitals have up to 87%. Compared with the $13a_g$ and $14a_g$ orbitals, the interaction of the π^* orbital of $Cr_2(O_2CH)_4$ with $(C_6H_6)_2$ is relatively small, and the Cr–C_6H_6 bond, therefore, may not be very strong. This is consistent with the Cr–Cr bond distance (2.256 Å) which is shorter than that in any other $Cr_2(O_2CR)_4L_2$ system (see Table 4.1.1 in ref 1).

To gain more insight into how the benzene–dichromium interactions would evolve at shorter distances, another calculation was performed. At a Cr–C_6H_6 distance of 2.3 Å, the calculated results for $Cr_2(O_2CH)_4(C_6H_6)_2$, as shown in Table X, are similar to those we discussed before. But, as expected, the interaction between the fragments has become stronger when they come closer. In addition to the interaction discussed before, the $4b_{2u}$ and $4b_{3u}$ orbitals of $(C_6H_6)_2$ now also interact strongly with the $6e_u$ (π) orbital of $Cr_2(O_2CH)_4$, which also generates two pairs of degenerate orbitals, namely, the $9b_{2u}/9b_{3u}$ pair and the $10b_{2u}/10b_{3u}$ pair. The contour plots for the $9b_{3u}$ and $10b_{3u}$ orbitals are shown in Figure 9 (parts a and b). It can be seen there that both pairs have Cr–Cr π bonding character, but one pair is Cr–C_6H_6 bonding and the other is Cr–C_6H_6 antibonding.

Comparing Table X with Table IX, it is found that all orbitals in Table X which have dominant chromium character have higher energy than the corresponding orbitals in Table IX. Obviously, when the benzene molecules are getting closer to $Cr_2(O_2CH_4)$, the very localized Cr–Cr orbitals in $Cr_2(O_2CH)_4$ are raised in energy. This makes it possible that the π orbital of $Cr_2(O_2CH)_4$ can interact with the benzene orbitals. Also because of this, the chromium atoms now have greater weight in the $14a_g$ orbital than in the $13a_g$ orbital, whereas the two orbitals have nearly equal weight when the Cr–C_6H_6 distance is large.

It seems that the interaction between the $5e_g$ (π^*) orbital and the orbitals of $(C_6H_6)_2$ is now more favorable spatially than energetically. When the fragments come closer, the interacting

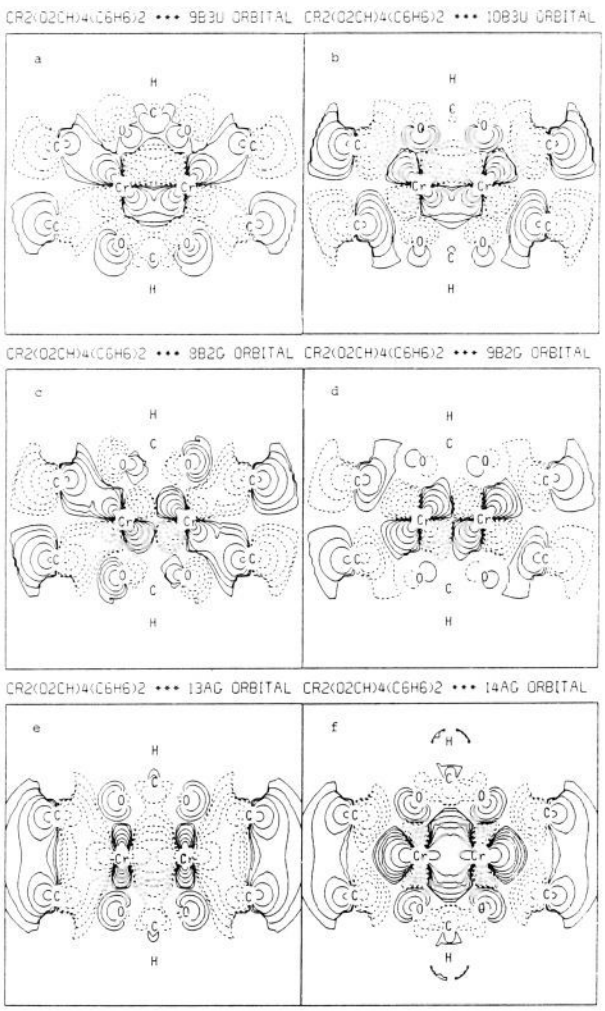

Figure 9. Contour plots of the $9b_{3u}$, $10b_{3u}$, $8b_{2g}$, $9b_{2g}$, $13a_g$, and $14a_g$ orbitals of $Cr_2(O_2CH)_4(C_6H_6)_2$ at a Cr–C_6H_6 distance of 2.3 Å.

orbitals overlap more effectively, which obviously increases the bonding effect between the fragments. But the rising of the π^* orbital in shortening the Cr–C_6H_6 distance is disfavored for the interaction. As a result, the energies of the $8b_{2g}$ and $8b_{3g}$ orbitals are lowered, indicating a stronger Cr–C_6H_6 bond than before, but the metal character in the orbitals which changed from 20% to 26% did not increase significantly. If one compares Figure 9c with Figure 8e, one finds that, while the overlap between the fragments is more effective for the shorter Cr–C_6H_6 distance, the Cr–Cr antibonding character in the two contours remains nearly the same. It might be said that the donation of electrons from the benzene molecules to the π^* orbital at the shorter Cr–C_6H_6 distance may not be more effective than at the longer distance. In saying this, one has to be aware of the fact that we are dealing with a completely hypothetic system, in which we let the benzene molecules move toward the $Cr_2(O_2CH)_4$ fragment without changing the geometry of the $Cr_2(O_2CH)_4$ unit. It would be expected in an "actual" case that closer approach of the benzene to $Cr_2(O_2CH)_4$ should cause some changes in the geometry of $Cr_2(O_2CH)_4$, say, lengthening the Cr–Cr bond distance. If so, the situation might be quite different from what we just discussed.

Compound 2. This compound consists of $Cr_2(O_2CCPh_3)_4py$ molecules packed in an unusual way. Apparently the packing forces are so dominated by the peripheral CPh_3 groups that the cavities available for axial ligation are, so to speak, "unsuitable" for normal pyridine coordination. Fist, there is nowhere nearly enough room for one pyridine molecule at each end of each $Cr_2(O_2CCPh_3)_4$ unit. In fact, there is not quite enough room for even one normally oriented pyridine molecule in each cavity, so

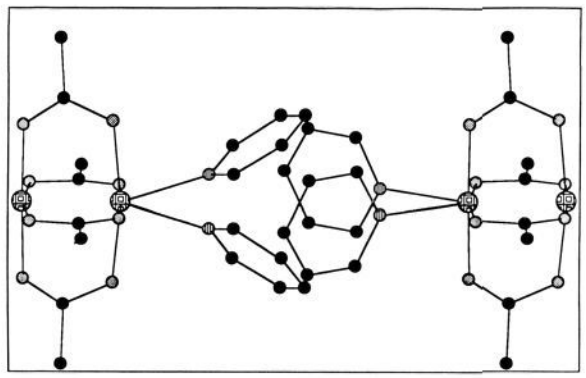

Figure 10. A ball and stick drawing showing how the systematic disordering of the pyridine molecules in compound **2** is modeled by placing four quarter pyridine molecules in each cavity.

that the one that is present adopts a slightly bent orientation. This can be seen in Figure 5. However, the midpoint of the cavity is a site of $\bar{4}$ crystallographic symmetry, and this leads to a form of systematic disorder. There are four possible locations for the pyridine molecule in each cavity, and over the many cavities in a macroscopic crystal one observes a random array. This gives the effect of having four quarter pyridine molecules per cavity, as shown in Figure 10.

The influence of the axially coordinated pyridine molecule on the Cr–Cr bond is surprisingly great. In previous studies[9] with other carboxylates and a variety of substituted pyridines (as well as py itself), we have found Cr–N distances in the range 2.23 and 2.39 Å, and thus the present one, 2.31 (4) Å, is typical, despite the tilt of the pyridine molecule. Even though there is only one axial pyridine ligand, the Cr–Cr distance, 2.383 (4) Å, is in the range, 2.30–2.50 Å, spanned by the dipyridinates. This would seem to imply that with a powerful base the first molecule has a decisive effect, leaving little further weakening of the Cr–Cr bond to be done by the second one. Unfortunately, this concept is no more than an ad hoc hypothesis since we have no other example of a monopyridinate of a $Cr_2(O_2CR)_4$ molecule.

In view of the dimensions of the cavity in compound **2** we considered that each cavity might be able to contain one pyrazine molecule, which could coordinate simultaneously to both neighboring dichromium molecules. Unfortunately, we have been unable, despite repeated attempts, to crystallize such a material.

Compound 3. Here we are on familiar ground, dealing with a $Cr_2(O_2CR)_4L_2$ molecule in which L is an oxygen atom donor. The results are, accordingly, unsurprising. The Cr–OEt_2 distance, 2.305 (14) Å, is similar to those in other molecules with R groups such as CH_3, CMe_3, H, or Ph and axial ligands such as H_2O, RCO_2H, or $CH_3OCH_2CH_2OCH_3$, namely 2.27–2.31 Å. The Cr–Cr distance, 2.303 (4) Å, is also comparable to the ones found before in such compounds, which were in the range 2.30–2.37 Å.

The unremarkable character of compound **3** is not unimportant: it shows that the $Cr_2(O_2CCPh_3)_4$ molecule, despite its exceptional steric properties, is not otherwise atypical of the entire class of $Cr_2(O_2CR)_4$ compounds and thus that its behavior in compounds **1** and **2** is pertinent to a general understanding of this class of compounds.

Acknowledgment. We thank the National Science Foundation for support.

Registry No. 1, 113055-80-4; **2**, 113055-81-5; **3**, 113055-82-6; $Cr_2(O_2CH)_4(C_6H_6)_2$, 113034-91-6; Cr, 7440-47-3; bis(cyclopentadienyl)-chromium, 1271-24-5.

Supplementary Material Available: Full listings of bond distances, bond angles, hydrogen atom positions, and anisotropic displacement parameters and packing diagram for compound **2** (30 pages); tables of calculated and observed structure factors for compounds **1–3** (32 pages). Ordering information is given on any current masthead page.